

## Two-level system in a bichromatic field

R. Guccione-Gush

4639 West 10th, Vancouver, British Columbia, Canada

H. P. Gush

Department of Physics, University of British Columbia, Vancouver, British Columbia, Canada

(Received 29 May 1974)

The behavior of a two-level system interacting with a bichromatic classical field is studied. Analytic expressions are found for the Green's-function operator for the system if the field is weak and near resonance, and a systematic procedure is developed to obtain the Green's-function operator in a more general case. The results are used to calculate the probability of a transition from the lower to the upper state; resonance conditions occur when the level spacing of the system,  $\omega_{b,a}$ , is near  $n\omega_\lambda - (n-1)\omega_\mu$ , where  $n$  is a positive or negative integer, and  $\omega_\lambda$  and  $\omega_\mu$  are the frequencies of the components of the field. The resonance frequency depends on the intensity of the field components. In addition, the cross section for scattering photons out of the field has been calculated. It is found that the spectrum of the scattered radiation consists of lines at frequency  $\omega_k = \omega_\mu, \omega_\lambda$ , and odd harmonics of these, combinations of the fundamental and the harmonics with  $\Delta = \omega_\lambda - \omega_\mu$ , and satellites shifted from all of these features by an amount which depends on the intensity of the field and  $\omega_{b,a}$ . The cross section is intensity dependent particularly insofar as the location of resonance peaks is concerned. It is suggested that this effect may be exploited in transferring intensity modulation of one component of the field to phase modulation in the other component.

### I. INTRODUCTION

The behavior of an atomic system in an intense electromagnetic field has become of considerable practical and theoretical interest as a result of the availability of powerful lasers. Because the field may rapidly induce large changes in the atomic wave function it is necessary, in order to calculate physical quantities of interest such as transition probabilities and scattering cross sections, to find, for example, the complete Green's-function operator of the system interacting with the field. To make this problem tractable, one is naturally forced to adopt some simplifying assumptions. The primary one adopted in this paper is that only two states of the atom are effective in its interaction with the radiation. That is, the atom is replaced by a two-level system endowed with an electric dipole moment. Furthermore, the energy levels are considered sharp, all relaxation processes being ignored.

The problem of a two-level system in a monochromatic field has been dealt with in some detail by several authors,<sup>1</sup> but the case of a bichromatic or polychromatic field has received much less attention because of its complexity. Although a general formalism to deal with these cases has been introduced by Chang and Stehle,<sup>2</sup> they did not treat examples. Using an entirely different approach, Mollow<sup>3</sup> has discussed a two-level system interacting with a pump field and a weak-signal field whose frequencies are very close to the resonance frequency of the atom. Two allied problems

to the one discussed here may also be mentioned: the spontaneous emission by a two-level atom into a multimode cavity, treated in the rotating-wave approximation by Swain<sup>4</sup>; and a three-level atom in the presence of a two-mode electromagnetic field, studied by Walls<sup>5</sup> and Chiarini *et al.*<sup>6</sup> Experiments involving the application of two oscillating fields to an atomic system have been carried out by Oka and collaborators.<sup>7</sup>

Whereas the problem of finding the Green's function of a two-level system in a monochromatic field could be solved by summing a perturbation series,<sup>1</sup> it does not appear to be possible to do this in general when another component is added to the field. However, if the two components of the field are relatively weak, and have a frequency which is near resonance, it is possible to sum the most important terms in the perturbation series, obtaining the Green's function in terms of continued fractions. The general case is attacked by postulating that the wave function of the two-level system in the bichromatic field has the form of a double Fourier series; the coefficients in this series satisfy certain recursion relations which permit their evaluation in principle. It is then shown that the Green's function may be expressed in terms of these coefficients.

From the Green's function, the probability of transition from the lower to the upper state may be evaluated, and several illustrative examples were calculated numerically. The two-level system displays nonlinearities, there being resonant transitions at sum and difference frequencies of the

two components of the field and significant intensity-dependent shifts in the resonance frequencies.

The cross section for the scattering of a photon out of the incident field has also been calculated. Here too, the system shows nonlinear effects, because, in addition to Rayleigh scattering, one finds photons emitted at sum and difference frequencies and satellite emission lines, the frequency of which depends on the field intensity. It is found that the scattering cross section depends on the field intensity, and this implies that the index of refraction of a gas of two-level atoms would be intensity dependent. This could have practical implications.

$$G^+(t-t_0) = G_0^+(t-t_0) + \hbar^{-1} \int dt' G_0^+(t-t') V(t') G_0^+(t'-t_0) + \hbar^{-2} \int \int dt' dt'' G_0^+(t-t') V(t') G_0^+(t'-t'') \times V(t'') G_0^+(t''-t_0) + \dots, \quad (2.2)$$

where  $G_0^+(t-t_0)$  is the zeroth-order Green's-function operator,

$$G_0^+(t-t_0) = -\lim_{\epsilon \rightarrow 0^+} \frac{1}{2\pi} \int_{-\infty}^{\infty} d\omega_1 \frac{e^{i\omega_1(t-t_0)}}{\omega_1 - i\epsilon} \times (|a\rangle\langle a| e^{-i\omega_a(t-t_0)} + |b\rangle\langle b| e^{-i\omega_b(t-t_0)}). \quad (2.3)$$

In (2.3) the lower and upper eigenstates of the unperturbed system,  $|a\rangle$  and  $|b\rangle$ , of eigenenergy  $\hbar\omega_a$  and  $\hbar\omega_b$ , respectively, have been introduced. In what follows the Green's-function operator will be expressed as the sum of four parts,

$$G^+ = G_{aa} + G_{bb} + G_{ab} + G_{ba}, \quad (2.4)$$

where

$$G_{ij} = -|i\rangle\langle j| e^{-i\omega_i(t-t_0)} \frac{1}{2\pi} \int d\omega_1 e^{i\omega_1(t-t_0)} \mathfrak{g}_{ij}(\omega_1). \quad (2.5)$$

The kernel  $\mathfrak{g}_{ij}(\omega_1)$  is the complete propagator of the two-level system interacting with the field.

It is assumed that the interaction of the system with the external field  $\vec{E}(t)$  takes place through the electric dipole moment  $\vec{d}$ , and the interaction potential equals

$$V(t) = -\vec{d} \cdot (\vec{E}_\lambda \cos \omega_\lambda t + \vec{E}_\mu \cos \omega_\mu t). \quad (2.6)$$

The matrix elements of  $V(t)$  are assumed real and are defined as follows:

$$\langle a|V|b\rangle = \langle b|V|a\rangle = 2\omega_c \hbar (\cos \omega_\lambda t + \alpha \cos \omega_\mu t), \quad (2.7)$$

where

$$\omega_c = -\langle a|\vec{d} \cdot \vec{E}_\lambda|b\rangle/2\hbar \quad (2.8)$$

## II. THEORETICAL BACKGROUND

The properties of a two-level system interacting with a classical field may be deduced from its Green's-function operator. This operator satisfies the equation

$$[H_0 + V(t) - i\hbar \partial/\partial t] G^+(t-t_0) = -\hbar\delta(t-t_0), \quad (2.1)$$

where  $H_0$  is the unperturbed Hamiltonian and  $V(t)$  is the interaction potential. The solution to (2.1) may be written in a perturbation series,

and

$$\alpha = \langle a|\vec{d} \cdot \vec{E}_\mu|b\rangle / \langle a|\vec{d} \cdot \vec{E}_\lambda|b\rangle. \quad (2.9)$$

When  $V(t)$  is introduced into (2.2) contributions to  $G^+$  result which can be interpreted as describing processes in which photons of type  $\lambda$  or type  $\mu$  are absorbed from or emitted into the field, although the latter is classical. The kernel  $\mathfrak{g}_{ij}$  may consequently be expressed as the sum of distinct contributions  $\mathfrak{g}_{ij}^{(N,M)}$ , corresponding to the net emission of  $N$   $\lambda$ -type photons and  $M$   $\mu$ -type photons. Of these contributions,  $\mathfrak{g}_{aa}^{(0,0)}$  has a special significance because it describes the process of forward scattering, that is, the propagation of the system in the ground state  $|a\rangle$  with no net emission or absorption of photons into the field. This forward scattering propagator has an expansion in terms of the self-energy  $\Sigma$  of the system:

$$\mathfrak{g}_{aa}^{(0,0)} = \mathfrak{g}_0 + \mathfrak{g}_0 \Sigma \mathfrak{g}_0 + \mathfrak{g}_0 \Sigma \mathfrak{g}_0 \Sigma \mathfrak{g}_0 + \dots, \quad (2.10)$$

where  $\mathfrak{g}_0$  is the unperturbed system propagator  $1/(\omega_1 - i\epsilon)$ . The self-energy  $\Sigma$  is the sum of all proper zero-net-photon-absorption diagrams, that is, those which do not contain  $\mathfrak{g}_0$ . The series (2.10) can be formally summed to yield

$$\mathfrak{g}_{aa}^{(0,0)} = 1/(\omega_1 - \Sigma - i\epsilon). \quad (2.11)$$

As will be shown later the general term  $\mathfrak{g}_{ij}^{(N,M)}$  is closely connected to  $\mathfrak{g}_{aa}^{(0,0)}$ , hence the determination of the self-energy is the first step in the calculation of  $G^+$ .

As a preliminary to the more complicated bichromatic case, the self-energy of the system is first found for the monochromatic case, that is, choosing  $\alpha$  equal to zero.

## A. Propagator for monochromatic case:

## Perturbation theory

A general term in the perturbation expansion for  $\mathfrak{g}_{ij}$  will be proportional to a product of factors of the type  $(\omega_1 - n\omega_\lambda - i\epsilon)^{-1}$ ,  $(\omega_1 + \omega_{ba} - m\omega_\lambda - i\epsilon)^{-1}$ , and  $\omega_c e^{\pm i\omega_\lambda t_0}$ , where  $\omega_{ba} = \omega_b - \omega_a$ . The former

$$\mathfrak{g}_{aa}^n(\omega_1) = \frac{\omega_c^2}{\omega_1 - i\epsilon} \left( \frac{e^{i2\omega_\lambda t_0}}{(\omega_1 + \omega_{ba} - \omega_\lambda - i\epsilon)(\omega_1 - 2\omega_\lambda - i\epsilon)} + \frac{1}{(\omega_1 + \omega_{ba} - \omega_\lambda - i\epsilon)(\omega_1 - i\epsilon)} \right. \\ \left. + \frac{1}{(\omega_1 + \omega_{ba} + \omega_\lambda - i\epsilon)(\omega_1 - i\epsilon)} + \frac{e^{-i2\omega_\lambda t_0}}{(\omega_1 + \omega_{ba} + \omega_\lambda - i\epsilon)(\omega_1 + 2\omega_\lambda - i\epsilon)} \right). \quad (2.12)$$

The second and third terms, to be identified with forward scattering processes, contribute to the second term of (2.10) and are represented by diagrams in Figs. 1(b) and 1(c). The central lines of these diagrams, that is, the propagators  $(\omega_1 + \omega_{ba} - \omega_\lambda - i\epsilon)^{-1}$  and  $(\omega_1 + \omega_{ba} + \omega_\lambda - i\epsilon)^{-1}$ , are the lowest-order contributions to the self-energy. The first and fourth terms, shown in Figs. 1(a) and 1(d), are contributions to  $\mathfrak{g}_{aa}^{(2)}$  and  $\mathfrak{g}_{aa}^{(-2)}$ , respectively.

It is convenient to normalize all frequencies in the problem to  $\omega_c$  and rename them as follows:  $\eta = \omega_1/\omega_c$ ,  $\eta' = (\omega_1 + \omega_{ba})/\omega_c$ , and  $\lambda = \omega_\lambda/\omega_c$ . Furthermore, the following compact notation is introduced:  $[m] = (\eta - m\lambda - i\epsilon)$ , if  $m$  is even;  $[m] = (\eta' - m\lambda - i\epsilon)$ , if  $m$  is odd; and  $[m, m \pm 1] = (\eta' - m\lambda - i\epsilon)[\eta - (m \pm 1)\lambda - i\epsilon]$ , if  $m$  is odd.

In higher order of perturbation theory more complicated contributions to  $\mathfrak{g}_{aa}$  and to  $\Sigma$  are found. Some examples of the latter are given in Fig. 2. All diagrams contributing to  $\Sigma$  can be divided into two classes, those beginning and ending with the propagator  $[+1]^{-1}$  ( $\Sigma^+$ ) and those beginning and ending with  $[-1]^{-1}$  ( $\Sigma^-$ ), where  $\Sigma = \Sigma^+ + \Sigma^-$ . It may be shown, following arguments developed in I, that

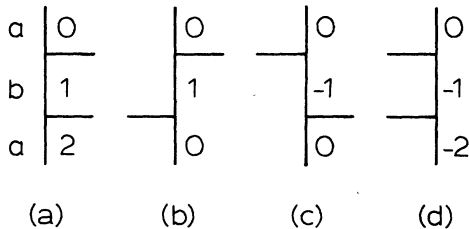


FIG. 1. Second-order diagrams contributing to  $\mathfrak{g}_{aa}$ . The letters  $a$  and  $b$  refer to the state of the two-level system, and the numbers refer to the integers  $n$  and  $m$  in the propagators  $(\omega_1 - n\omega_\lambda - i\epsilon)^{-1}$  and  $(\omega_1 + \omega_{ba} - m\omega_\lambda - i\epsilon)^{-1}$ , where  $n$  is even and  $m$  is odd.

two factors are propagators and the latter factors are vertex contributions. Referring to a description of the perturbation series using diagrams, the integers  $n$  and  $m$  indicate the number of photons emitted above the corresponding propagator. For example, the second-order contribution to  $\mathfrak{g}_{aa}$  is the following sum of four terms:

$$\Sigma^- = \frac{1}{[-1]} \sum_{m_1, m_2, \dots=0}^{\infty} \left( \frac{1}{[-2, -1]} \right)^{m_1} \binom{m_1 + m_2 - 1}{m_2} \\ \times \left( \frac{1}{[-2, -3]} \right)^{m_2} \binom{m_2 + m_3 - 1}{m_3} \left( \frac{1}{[-4, -3]} \right)^{m_3} \dots \\ = \frac{1}{\eta' + \lambda - i\epsilon} - \frac{1}{\eta + 2\lambda - i\epsilon} - \frac{1}{\eta' + 3\lambda - i\epsilon} - \dots, \quad (2.13)$$

and

$$\Sigma^+ = \frac{1}{[+1]} \sum_{m_1, m_2, \dots=0}^{\infty} \left( \frac{1}{[2, 1]} \right)^{m_1} \binom{m_1 + m_2 - 1}{m_2} \\ \times \left( \frac{1}{[2, 3]} \right)^{m_2} \binom{m_2 + m_3 - 1}{m_3} \left( \frac{1}{[4, 3]} \right)^{m_3} \dots \\ = \frac{1}{\eta' - \lambda - i\epsilon} - \frac{1}{\eta - 2\lambda - i\epsilon} - \frac{1}{\eta' - 3\lambda - i\epsilon} - \dots. \quad (2.14)$$

The zero-photon-emission propagator in the monochromatic case equals

$$\mathfrak{g}_{aa}^{(0)} = 1/(\eta - \Sigma^+ - \Sigma^- - i\epsilon). \quad (2.15)$$

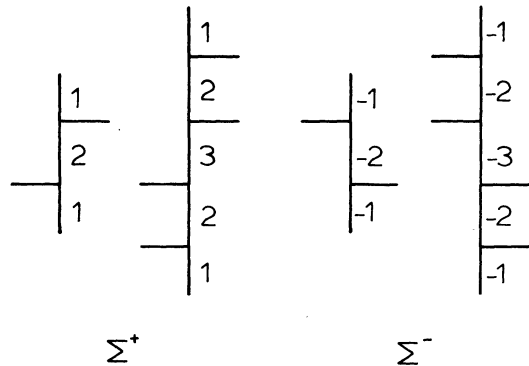


FIG. 2. Second- and fourth-order contributions to the components  $\Sigma^+$  and  $\Sigma^-$  of the self-energy.

Introducing (2.13) and (2.14) into (2.15) one obtains an expression for  $g_{aa}^{(0)}$  in terms of continued fractions identical to that in I, equation (2.14), obtained without recourse to the notion of self-energy.

As mentioned previously, not only is  $g_{aa}^{(0)}$  determined by the self-energy, but so are those parts of  $g_{ij}$  involving the net emission or absorption of photons. For example, consider the propagator which takes the system from the state  $|b\rangle$  to the state  $|a\rangle$  with the net emission of one photon. This propagator may be visualized by means of graphs shown in Fig. 3. It is clear from the construction of Fig. 3(b) that the lower blob in Fig. 3(c) is none other than  $\Sigma^+$ . For, if a free propagator had appeared in the lower part of the diagram, the resulting graph would contain a repetition of a graph already contained in  $g_{aa}^{(0)}$ . Hence

$$g_{ab}^{(1)} = -g_{aa}^{(0)} \Sigma^+ e^{i\omega\lambda t_0}, \quad (2.16)$$

and, similarly,

$$g_{ab}^{(-1)} = -g_{aa}^{(0)} \Sigma^- e^{-i\omega\lambda t_0}. \quad (2.17)$$

Furthermore, a propagator which takes the system from state  $|a\rangle$  to state  $|a\rangle$ , but in which, for example, a net number of two photons is emitted, can be obtained multiplying  $g_{ab}^{(1)}$  by the sum of all zero-net-photon-emission diagrams which do not contain either  $[0]$  or  $[+1]$ . That is,

$$g_{aa}^{(2)} = g_{ab}^{(1)} \Lambda e^{i\omega\lambda t_0}, \quad (2.18)$$

where

$$\Lambda = \frac{1}{[2]} \sum_{m_1, m_2, \dots = 0}^{\infty} \left( \frac{1}{[3, 2]} \right)^{m_1} \binom{m_1 + m_2 - 1}{m_2} \times \left( \frac{1}{[3, 4]} \right)^{m_2} \dots \quad (2.19)$$

is a constituent of  $\Sigma^+$ . In a similar way contribu-

tions to  $g_{ij}$  involving an arbitrary number of photons can be built up.

### B. Wave function and Floquet's theorem

The wave function  $|\psi(t)\rangle$  of the system results from operating on the initial state with  $G^+$ . Suppose, for example, that at time  $t_0=0$  the initial state is  $|a\rangle$ , then

$$\begin{aligned} |\psi(t)\rangle &= G^+(t)|a\rangle \\ &= -|a\rangle e^{-i\omega_a t} \frac{1}{2\pi} \int d\eta e^{i\omega_c \eta t} g_{aa}(\eta) \\ &\quad - |b\rangle e^{-i\omega_b t} \frac{1}{2\pi} \int d\eta e^{i\omega_c \eta t} g_{ba}(\eta). \end{aligned} \quad (2.20)$$

As was shown in I the poles of  $g_{aa}$  and  $g_{ba}$  are located at

$$\eta_p = -\frac{1}{2}\gamma + l\zeta + 2m\lambda \quad (2.21a)$$

and

$$\eta_p = \frac{1}{2}\gamma + l\zeta + 2m\lambda, \quad (2.21b)$$

respectively, where  $\gamma = (\omega_{ba} - \omega_\lambda)/\omega_c$ ,  $l = \pm 1$ ,  $m$  is a positive or negative integer, and  $\zeta$  is a parameter which depends on  $\lambda$  and  $\delta = \omega_{ba}/\omega_c$ . Denoting the residues of  $g_{aa}$  and  $g_{ba}$  by  $R(aa|lm)$  and  $R(ba|lm)$ , respectively, one may write

$$\begin{aligned} |\psi(t)\rangle &= -i \left[ \sum_l \exp[i(-\frac{1}{2}\gamma\omega_c + l\zeta\omega_c - \omega_a)t] \right. \\ &\quad \times \left( |a\rangle \sum_m R(aa|lm) e^{i2m\omega_\lambda t} \right. \\ &\quad \left. \left. + |b\rangle \sum_m R(ba|lm) e^{i(2m-1)\omega_\lambda t} \right) \right]. \end{aligned} \quad (2.22)$$

This result suggests that one could write for a general wave function the expression

$$|\psi(t)\rangle = e^{i\chi t} \left( |a\rangle \sum_m A_m e^{-im\omega_\lambda t} + |b\rangle \sum_n B_n e^{-in\omega_\lambda t} \right), \quad (2.23)$$

where  $\chi$  is a parameter. Indeed, reducing Schrödinger's equation

$$(H_0 + V(t))|\psi(t)\rangle = i\hbar \dot{|\psi(t)\rangle} \quad (2.24)$$

to a Hill's equation (which is possible here) and then invoking Floquet's theorem,<sup>8</sup> one is led to postulate for the wave function of the system the form (2.23). This procedure was used by Autler and Townes.<sup>9</sup>

The close connection between the parameter  $\chi$  and the poles of the complete propagator suggests a possible approach to determining the Green's-function operator without recourse to perturbation

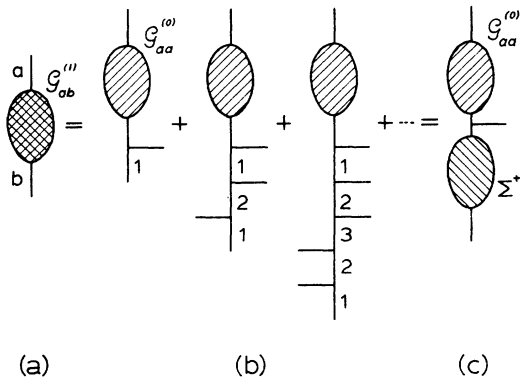


FIG. 3. Graphs representing the one-photon-emission contributions to  $g_{ab}$ .

theory. Clearly, in order that (2.23) be a solution to (2.24)  $\chi$  may assume only certain allowed values. Suppose that the relation which yields the values of  $\chi$  has the form  $\chi - F(\chi) = 0$ . Then the self-energy of the system is, to within an additive constant, none other than  $F(\chi)$ , and  $g_{aa}^{(0)}$  must be equal to  $1/[\chi - F(\chi)]$ . This turns out to be a more powerful way to obtain the Green's-function operator than by summation of the perturbation series.

The relation which must be satisfied by  $\chi$  is found by substituting (2.23) into the Schrödinger equation (2.24) and multiplying from the left with  $\langle a|$  and  $\langle b|$ . One finds that

$$(\chi + \omega_a - n\omega_\lambda)A_n = -\omega_c(B_{n-1} + B_{n+1}) \quad (2.25a)$$

and

$$(\chi + \omega_b - n\omega_\lambda)B_n = -\omega_c(A_{n-1} + A_{n+1}). \quad (2.25b)$$

In particular, from (2.25a) with  $n=0$  one has

$$(\chi + \omega_a)/\omega_c + B_{-1}/A_0 + B_{+1}/A_0 = 0. \quad (2.26)$$

The ratios  $B_{-1}/A_0$  and  $B_{+1}/A_0$  are obtained by systematic elimination of unknowns from Eqs. (2.25):

$$B_{-1}/A_0 = \frac{-1}{\eta' + \lambda} - \frac{1}{\eta + 2\lambda} - \frac{1}{\eta' + 3\lambda} - \dots = -\Sigma^-, \quad (2.27)$$

$$B_{+1}/A_0 = \frac{-1}{\eta' - \lambda} - \frac{1}{\eta - 2\lambda} - \frac{1}{\eta' - 3\lambda} - \dots = -\Sigma^+.$$

In Eqs. (2.27) the variables  $\eta = (\chi + \omega_a)/\omega_c$  and  $\eta' = (\chi + \omega_b)/\omega_c$  have been introduced. Substituting in (2.26) the expressions for  $B_{-1}/A_0$  and  $B_{+1}/A_0$  given by (2.27) one obtains the denominator of the propagator (2.15), and one sees that the self-energy equals the sum of  $-B_{-1}/A_0$  and  $-B_{+1}/A_0$ . Referring to equations (2.16) and (2.17) one may write that

$$g_{ab}^{(1)} = g_{aa}^{(0)}(B_{+1}/A_0)e^{i\omega_\lambda t_0}, \quad (2.28)$$

$$g_{ab}^{(-1)} = g_{aa}^{(0)}(B_{-1}/A_0)e^{-i\omega_\lambda t_0}, \quad (2.29)$$

and furthermore it may be shown that

$$g_{aa}^{(N)} = g_{aa}^{(0)}(A_N/A_0)e^{iN\omega_\lambda t_0}, \quad N \text{ even}, \quad (2.30a)$$

and

$$g_{ab}^{(N)} = g_{aa}^{(0)}(B_N/A_0)e^{iN\omega_\lambda t_0}, \quad N \text{ odd}. \quad (2.30b)$$

It follows that the entire Green's-function operator can be built up from the coefficients  $A_n$  and  $B_n$ .

### III. BICHROMATIC CASE

Except for a special case, to be discussed shortly, where the bichromatic problem can be solved with both the perturbation theory approach and the Floquet-theorem approach, it is necessary to attack the bichromatic case using the method outlined at the end of Sec. II.

As a trial wave function a simple generalization of Eq. (2.23) is postulated:

$$|\psi\rangle = e^{i\chi t} \left( |a\rangle \sum_{n,m} A_{nm} e^{-i(n\omega_\lambda + m\omega_\mu)t} + |b\rangle \sum_{n,m} B_{nm} e^{-i(n\omega_\lambda + m\omega_\mu)t} \right). \quad (3.1)$$

By introducing (3.1) into (2.24) and projecting respectively on  $\langle a|$  and  $\langle b|$  one obtains the following conditions on the expansion coefficients  $A_{nm}$  and  $B_{nm}$ :

$$(\eta - n\lambda - m\mu)A_{nm} = -(B_{n-1,m} + B_{n+1,m}) - \alpha(B_{n,m-1} + B_{n,m+1}), \quad (3.2a)$$

$$(\eta' - n\lambda - m\mu)B_{nm} = -(A_{n-1,m} + A_{n+1,m}) - \alpha(A_{n,m-1} + A_{n,m+1}), \quad (3.2b)$$

where the variables  $\eta = (\chi + \omega_a)/\omega_c$  and  $\eta' = (\chi + \omega_b)/\omega_c$  and the parameters  $\lambda = \omega_\lambda/\omega_c$  and  $\mu = \omega_\mu/\omega_c$  have been introduced. In particular, if  $n$  and  $m$  are set equal to zero in (3.2a) one obtains the relation

$$\eta + (B_{-10} + B_{10} + \alpha B_{0-1} + \alpha B_{01})/A_{00} = 0. \quad (3.3)$$

Following the arguments of the previous section one is led to postulate for the zero-photon-absorption propagator the expression

$$g_{aa}^{(0,0)} = [\eta + (B_{-10} + B_{10} + \alpha B_{0-1} + \alpha B_{01})/A_{00} - i\epsilon]^{-1}. \quad (3.4)$$

At first sight it is not at all obvious how to solve Eqs. (3.2) because there is no *a priori* reason that one coefficient or group of coefficients is more important than another. Furthermore, direct numerical solution with a computer is restricted to a relatively small number of coefficients. As a guide to solving for the  $A_{nm}$  and  $B_{nm}$  in an arbitrary case, it will first be assumed that both components of the field are weak and near resonance with the two-level system. This is a case which can be solved both in perturbation theory and using the Floquet's theorem approach. It is found that there is a close connection between the propagators obtained in perturbation theory and the coefficients obtained from (3.2). This connection, which we assume can be generalized to an arbitrary case, is

$$g_{aa}^{(N,M)} = g_{aa}^{(0,0)}(A_{NM}/A_{00})e^{i(N\omega_\lambda + M\omega_\mu)t_0}, \quad N+M \text{ even}, \\ g_{ab}^{(N,M)} = g_{aa}^{(0,0)}(B_{NM}/A_{00})e^{i(N\omega_\lambda + M\omega_\mu)t_0}, \quad N+M \text{ odd}. \quad (3.5)$$

These relations are extensions of Eqs. (2.30).

Referring to Eqs. (3.5), it is seen that the proba-

bility that the two-level system makes a transition from, for example, state  $|a\rangle$  to state  $|a\rangle$ , emitting  $N$   $\lambda$ -type photons and  $M$   $\mu$ -type photons into the field depends intimately on  $A_{NM}$ . This interpretation of the coefficients assists in judging which ones might be the most significant in a particular problem. For example, for the near resonance case cited above only coefficients of the type  $A_{N,-N}$  and  $B_{N,-N+1}$  will be important, these corresponding to nearly energy-conserving processes. In this way one has a physical argument for focusing one's attention on a restricted group of coefficients.

### A. Ladder approximation

#### 1. Perturbation-theory treatment

In the case that the frequencies  $\omega_\lambda$  and  $\omega_\mu$  are close to  $\omega_{ba}$  and the field is weak only a certain class of diagrams is important, and they can be counted, in contrast to the general case. These have the appearance of a ladder, in which a photon absorption is followed by a photon emission, and vice versa, and in which for  $\mathcal{G}_{aa}$ , for example, the first interaction is an absorption. A diagram of this class hence consists of a sequence of nearly unperturbed propagators. This is an extension of the rotating-wave approximation of the monochromatic case.

Consider now diagrams in which the number of photons emitted minus the number of photons absorbed of either type equals zero. The second order ladder contribution to the system propagator from these processes equals

$$\begin{aligned} \Sigma_\lambda^+ &= \frac{1}{[\lambda]} \sum_{n_1, n_2, \dots = 0} \left( \frac{\alpha^2}{[\lambda - \mu, \lambda]} \right)^{n_1} \binom{n_1 + n_2 - 1}{n_2} \left( \frac{1}{[\lambda - \mu, 2\lambda - \mu]} \right)^{n_2} \binom{n_2 + n_3 - 1}{n_3} \left( \frac{\alpha^2}{[2\lambda - 2\mu, 2\lambda - \mu]} \right)^{n_3} \dots \\ &= \frac{1}{\eta' - \lambda - i\epsilon - \frac{\alpha^2}{\eta' - \lambda + \mu - i\epsilon} - \frac{1}{\eta' - 2\lambda + \mu - i\epsilon} - \frac{\alpha^2}{\eta' - 2\lambda + 2\mu - i\epsilon} - \dots}, \end{aligned} \quad (3.8)$$

and

$$\begin{aligned} \Sigma_\mu^+ &= \frac{\alpha^2}{[\mu]} \sum_{n_1, n_2, \dots = 0} \left( \frac{1}{[-\lambda + \mu, \mu]} \right)^{n_1} \binom{n_1 + n_2 - 1}{n_2} \left( \frac{\alpha^2}{[-\lambda + \mu, -\lambda + 2\mu]} \right)^{n_2} \binom{n_2 + n_3 - 1}{n_3} \left( \frac{1}{[-2\lambda + 2\mu, -\lambda + 2\mu]} \right)^{n_3} \dots \\ &= \frac{\alpha^2}{\eta' - \mu - i\epsilon - \frac{1}{\eta' + \lambda - \mu - i\epsilon} - \frac{\alpha^2}{\eta' + \lambda - 2\mu - i\epsilon} - \frac{1}{\eta' + 2\lambda - 2\mu - i\epsilon} - \dots}. \end{aligned} \quad (3.9)$$

We note that  $\Sigma_\lambda^+$  and  $\Sigma_\mu^+$  consist of products of propagators  $[n\lambda + m\mu]^{-1}$ , with  $n + m = 0$  and  $n + m = 1$ , only.

The zero-photon-emission propagator consequently equals,

$$\mathcal{G}_{aa}^{(0,0)} = 1/(\eta - \Sigma_\lambda^+ - \Sigma_\mu^+ - i\epsilon). \quad (3.10)$$

The rotating-wave approximation to  $\mathcal{G}_{aa}$  for the

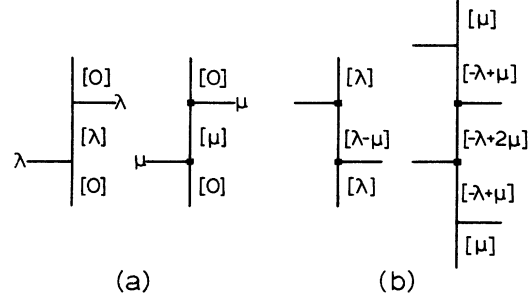


FIG. 4. (a) Second-order ladder diagrams contributing to  $\mathcal{G}_{aa}^{(0,0)}$ . The square vertex indicates absorption or emission of a  $\mu$ -type photon. (b) Examples of self-energy diagrams.

$$\mathcal{G}_{aa}^{(0,0)''} = \frac{1}{\eta - i\epsilon} \left( \frac{1}{\eta' - \lambda - i\epsilon} + \frac{\alpha^2}{\eta' - \mu - i\epsilon} \right) \frac{1}{\eta - i\epsilon}. \quad (3.6)$$

Graphs corresponding to Eq. (3.6) are shown in Fig. 4(a), where the following compact notation for reciprocal propagators has been introduced:  $[n\lambda + m\mu] = (\eta - n\lambda - m\mu - i\epsilon)$ ,  $n + m$  even;  $[n\lambda + m\mu] = (\eta' - n\lambda - m\mu - i\epsilon)$ ,  $n + m$  odd; and  $[n\lambda + m\mu, (n \pm 1)\lambda + m\mu] = [n\lambda + m\mu][n \pm 1)\lambda + m\mu]$ .

As in the monochromatic case, to obtain  $\mathcal{G}_{aa}^{(0,0)}$  we now sum the self-energy diagrams only. Of these there are two classes, those commencing and ending with  $[\lambda]^{-1}$  and  $[\mu]^{-1}$ , respectively. Some examples are shown in Fig. 4(b). The self-energy in the ladder approximation may hence be written

$$\Sigma^+ = \Sigma_\lambda^+ + \Sigma_\mu^+, \quad (3.7)$$

where

monochromatic case is obtained by putting  $\alpha$  equal to zero in (3.10). That is,

$$\mathcal{G}_{aa}^{(0)} = 1/(\eta - i\epsilon - 1/(\eta' - \lambda - i\epsilon)), \quad (3.11)$$

in agreement with Eq. (2.22a) of I. On the basis of Eq. (3.11) one might have guessed that the propagator for the bichromatic case in the rotating-wave approximation would have the form,

$$g_{aa}^{(0,0)} \approx [\eta - i\epsilon - 1/(\eta' - \lambda - i\epsilon) - \alpha^2/(\eta' - \mu - i\epsilon)]^{-1}. \quad (3.12)$$

However, this guess is seriously in error. Numerical analysis of Eq. (3.10) reveals that the continued fractions which follow  $1/(\eta' - \lambda - i\epsilon)$  and  $\alpha^2/(\eta' - \mu - i\epsilon)$  in Eqs. (3.8) and (3.9), respectively, have a profound effect on the pole locations and residues of  $g_{aa}^{(0,0)}$ . This is because  $\lambda - \mu$  is assumed a small quantity. Equation (3.12) results from considering those ladder diagrams which

contain only the propagators  $[0]^{-1}$ ,  $[\lambda]^{-1}$ , and  $[\mu]^{-1}$ , that is, diagrams where every other propagator is  $[0]^{-1}$ .<sup>10</sup>

We next consider contributions to the system propagator arising from diagrams in which, for example, there is a net emission of one  $\lambda$ -type photon and a net absorption of one  $\mu$ -type photon. Although energy is not conserved, these diagrams are nevertheless significant because of the closeness of  $\mu$  and  $\lambda$ . Two typical diagrams are shown in Fig. 5. Summing all those diagrams which do not contain a free propagator one has

$$\begin{aligned} \Sigma^{(1,-1)} &= \frac{\alpha}{[\lambda, \lambda - \mu]} \sum_{n_1, n_2, \dots = 0}^{\infty} \left( \frac{\alpha^2}{[\lambda, \lambda - \mu]} \right)^{n_1} \binom{n_1 + n_2}{n_2} \left( \frac{1}{[2\lambda - \mu, \lambda - \mu]} \right)^{n_2} \binom{n_2 + n_3 - 1}{n_3} \left( \frac{\alpha^2}{[2\lambda - \mu, 2\lambda - 2\mu]} \right)^{n_3} \dots \\ &= \left( \frac{\alpha}{[\lambda - \mu]} - \frac{1}{[2\lambda - \mu]} - \frac{\alpha^2}{[2\lambda - 2\mu]} - \dots \right) \left( \frac{1}{[\lambda]} - \frac{\alpha^2}{[\lambda - \mu]} - \frac{1}{[2\lambda - \mu]} - \dots \right) \end{aligned} \quad (3.13)$$

and

$$g_{aa}^{(1,-1)} = g_{aa}^{(0,0)} \Sigma^{(1,-1)} e^{i(\omega_\lambda - \omega_\mu)t_0}. \quad (3.14)$$

This procedure can be readily extended to calculate  $g_{aa}^{(N,-N)}$  for arbitrary  $N$ . There are no other contributions to  $g_{aa}$  in the ladder approximation.

The propagator involving the net absorption or emission of photons can be obtained using the same method outlined in Sec. II. It is readily shown that, for example,

$$g_{ab}^{(1,0)} = -g_{aa}^{(0,0)} \Sigma_\lambda^+ e^{i\omega_\lambda t_0}. \quad (3.15)$$

The poles of  $g_{ab}^{(1,0)}$  are the same as those of  $g_{aa}^{(0,0)}$ , which follows from the form of (3.15), the properties of  $g_{aa}^{(0,0)}$ , Eq. (3.10), and  $\Sigma_\lambda^+$ , Eq. (3.9).

The propagators  $g_{bb}^{(N,-N)}$  and  $g_{ba}^{(N,-N-1)}$  are obtained from  $g_{aa}^{(-N,N)}$  and  $g_{ab}^{(-N,N+1)}$  by exchanging

$a$  with  $b$  everywhere and replacing  $\lambda$  and  $\mu$  with  $-\lambda$  and  $-\mu$ .

## 2. Floquet's-theorem approach

As has already been stated, to obtain the Green's-function operator using the Floquet's-theorem approach it is necessary to solve Eqs. (3.2) for the coefficients  $B_{-10}$ ,  $B_{10}$ ,  $B_{0-1}$ , and  $B_{01}$ . Because the factors on the left of Eqs. (3.2),  $(\eta - n\lambda - m\mu)$  and  $(\eta' - n\lambda - m\mu)$ , have formally the appearance of reciprocals of propagators, to obtain an expression for  $g_{aa}^{(0,0)}$  similar to the one obtained in perturbation theory one must set equal to zero all coefficients  $A_{nm}$  with  $n+m \neq 0$  and all coefficients  $B_{nm}$  with  $n+m \neq 1$ . The connection between the perturbation theory approach and this approach is in fact the following. If, in the perturbation theory, one takes into account all propagators up to some maximum,  $n=N$  and  $m=M$ , then to obtain an equivalent result here one must include all coefficients up to  $A_{NM}$  or  $B_{NM}$ . With these simplifications the set of equations (3.2) can be solved by iteration, and one finds,

$$\frac{B_{10}}{A_{00}} = - \left( \frac{1}{\eta' - \lambda} - \frac{\alpha^2}{\eta' - \lambda + \mu} - \frac{1}{\eta' - 2\lambda + \mu} - \dots \right) = -\Sigma_\lambda^+, \quad (3.16a)$$

$$\begin{aligned} \frac{B_{01}}{A_{00}} &= - \left( \frac{\alpha}{\eta' - \mu} - \frac{1}{\eta' + \lambda - \mu} - \frac{\alpha^2}{\eta' + \lambda - 2\mu} - \dots \right) \\ &= -\frac{1}{\alpha} \Sigma_\mu^+, \end{aligned} \quad (3.16b)$$

$$B_{-10} = B_{0-1} = 0. \quad (3.16c)$$

If these relations are introduced into Eq. (3.4) one

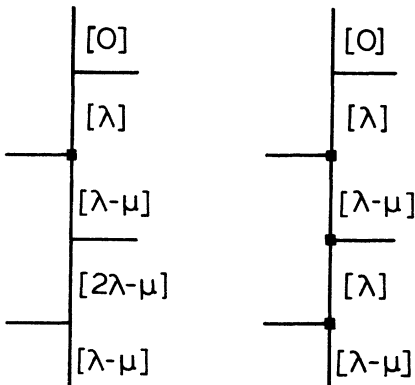


FIG. 5. Examples of ladder diagrams contributing to  $g_{aa}^{(1,-1)}$ .

obtains a propagator identical to that given by Eq. (3.10). Moreover, an inspection of Eqs. (3.15) and (3.16a) reveals that the propagator  $g_{ab}^{(1,0)}$  is simply related to  $B_{10}$ . In fact,

$$g_{ab}^{(1,0)} = g_{aa}^{(0,0)}(B_{10}/A_{00})e^{i\omega_\lambda t_0}. \quad (3.17)$$

Concurrently with the solution for  $B_{10}$  one finds an expression for  $A_{1-1}$ :

$$\begin{aligned} \frac{A_{1-1}}{A_{00}} &= \left( \frac{\alpha}{\eta - \lambda + \mu - \eta' - 2\lambda + \mu - \eta - 2\lambda + 2\mu - \dots} \right) \\ &\times \left( \frac{1}{\eta' - \lambda - \eta - \lambda + \mu - \eta' - 2\lambda + \mu - \dots} \right), \end{aligned} \quad (3.18)$$

and it is seen that  $A_{1-1}/A_{00}$  is identical to  $\Sigma^{(1,-1)}$ , defined in Eq. (3.13). It follows, therefore, that

$$g_{aa}^{(1,-1)} = g_{aa}^{(0,0)}(A_{1-1}/A_{00})e^{i(\omega_\lambda - \omega_\mu)t_0}. \quad (3.19)$$

These results make it plausible that in general the propagators corresponding to the absorption or emission of any arbitrary number of photons have the form specified in Eq. (3.5).

### 3. Applications

The Green's-function operator can be used, for example, to calculate the probability that a two-level system, suddenly immersed in the field, makes a transition from the lower to the upper state

$$\begin{aligned} W_{ba} &= 1 - |\langle a | G^+(t-t_0) | a \rangle|^2 \\ &= 1 - \left| \frac{1}{2\pi} \int d\eta e^{i\eta\omega_c(t-t_0)} g_{aa}(\eta) \right|^2. \end{aligned} \quad (3.20)$$

To evaluate  $W_{ba}$  it is clear that one requires the poles and residues of  $g_{aa}$ . These have been obtained by numerical analysis on a digital computer.

In practice, the continued fractions in (3.16a) and (3.16b) are terminated at a certain level. The depth to which one must go depends on the value of  $\lambda - \mu$  and is determined empirically. That is, in the computation, the depth is systematically increased until the addition of a new layer makes no significant difference in the pole locations and in the residues. Certain checks were applied to the residues obtained. In particular, the sum over all the poles of the residues of  $g_{aa}^{(n,-n)}$  equalled unity for  $n=0$ , and equalled zero for  $n \neq 0$ . Also the sum of the residues of  $g_{ba}^{(n,-n-1)}$  equalled zero, and the sum of the squares of the residues of  $g_{aa}$  and  $g_{ba}$  equalled unity.

It is found that the poles of  $g_{aa}^{(0,0)}$  are located at

$$P_{m\ell}^a = -\frac{1}{2}\gamma + l\xi + m\Delta, \quad (3.21)$$

where  $\gamma = (\omega_{ba} - \omega_\mu)/\omega_c$ ,  $\Delta = \lambda - \mu$ ,  $m$  is a positive or

negative integer, and  $l$  has the values  $\pm 1$ . The quantity  $\xi$  must be determined for each choice of  $\lambda$ ,  $\mu$ ,  $\alpha$ , and  $\delta = \omega_{ba}/\omega_c$ . A typical set of pole locations along the  $\eta$  axis is shown in Fig. 6. The location of the poles of  $g_{aa}$  as a function of  $\delta$  is shown in Fig. 7 for the case  $\lambda=100$ ,  $\mu=98$ , and  $\alpha=1, 0.5$ , and  $0.1$ . As seen in the figure there are values of  $\delta$  for which the poles approach each other closely; these define resonance conditions in  $\omega_{ba}$ .

Denoting the residues of  $g_{aa}^{(n,-n)}$  by the symbol  $R_{m\ell n}$ , the probability (3.20) can be expressed in the following way:

$$W_{ba} = 1 - \left| \sum_{m,\ell,n} R_{m\ell n} \exp[i\omega_c P_{m\ell}^a(t-t_0)] \exp[in\Delta t_0] \right|^2. \quad (3.22)$$

The time-independent part of  $W_{ba}$  equals the average probability  $W'_{ba}$  that the system be in the state  $|b\rangle$  having started at an uncertain time in state  $|a\rangle$ :

$$W'_{ba} = 1 - \sum_{m,\ell,n} |R_{m\ell n}|^2. \quad (3.23)$$

In Fig. 8 six curves of  $W'_{ba}$  are plotted as a function of  $\delta$  for the case  $\lambda=100$ . In Figs. 8(a), 8(c), and 8(d) the value of  $\alpha$  has been chosen to be unity, and the values of  $\mu$  have been chosen equal to 90, 97, and 98, respectively.<sup>11</sup> The curve corresponding to  $\mu=90$  was in fact calculated using a procedure to be described later, because the ladder approximation is not valid for such a large separation between  $\mu$  and  $\lambda$ . It is included here in order to aid in the interpretation of the resonance peaks. Referring to this case,  $W'_{ba}$  consists of two broad features centered near  $\delta=90$  and  $\delta=100$ , and two sharp peaks near  $\delta=80.28$  and  $\delta=109.7$ . The broad peaks correspond to absorption of single  $\mu$ -type photons and single  $\lambda$ -type photons, respectively. The sharp peak at  $\delta=80.28$  corresponds to the absorption of two  $\mu$ -type photons and the emission of one  $\lambda$ -type photon, whereas the one at  $\delta=109.7$  corresponds to the absorption of two  $\lambda$ -type photons and the emission of a  $\mu$ -type photon. In the case of  $\mu=97$  the two multiphoton peaks have shifted to  $\delta \approx 95$  and  $102$ , respectively, whereas the two main

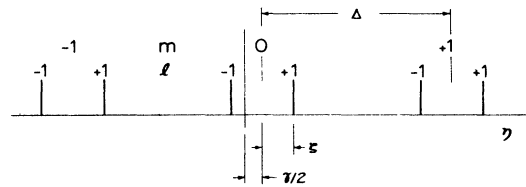


FIG. 6. Illustrating the pole locations of  $g_{aa}$ .

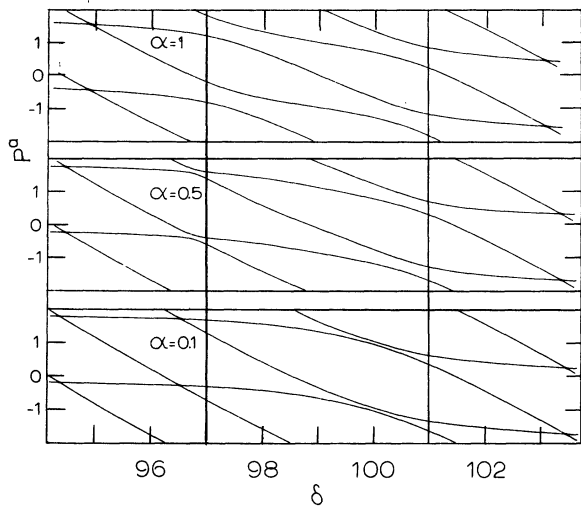


FIG. 7. Pole locations of  $G_{aa}$  as a function of  $\delta$  for the case  $\lambda=100$  and  $\mu=98$ . Three cases are shown corresponding to values of  $\alpha$  equal to 1, 0.5, and 0.1.

peaks due to absorption of single  $\lambda$ - and  $\mu$ -type photons have coalesced into one broad feature centered at  $\delta=98.5$ . Two other sharp features are included in the figure, at  $\delta=105.4$  and  $\delta=91.6$ ,

due to processes in which three  $[\lambda(\mu)]$ -type photons are absorbed and two  $[\mu(\lambda)]$ -type photons are emitted. Finally, for  $\mu=98$ , the two peaks due to  $(2\lambda - \mu)$ - and  $(2\mu - \lambda)$ -processes almost completely overlap the central feature due to single  $\lambda$ - and  $\mu$ -type absorption. One would have probably incorrectly identified all the peaks in this graph had a comparison with the cases  $\mu=97$  and  $\mu=90$  not been available. This is because the peaks occur at frequencies which are closer to the central value of the spectrum,  $\delta = \frac{1}{2}(\lambda + \mu)$ , than one would expect.

We remark that if  $W'_{ba}$ , calculated in the ladder approximation, is plotted as a function of  $\xi = \delta - \frac{1}{2}(\lambda + \mu)$ , distinct curves are obtained only for distinct values of  $\lambda - \mu$ . In other words, Fig. 8(d) represents  $W'_{ba}$  for all cases  $\lambda - \mu = 2$ .

Figures 8(e) and 8(f) illustrate the cases  $\lambda=100$ ,  $\mu=98$ , in which  $\alpha$  has the values 0.5 and 0.1, respectively. The main feature of Fig. 8(f) is a broad resonance centered at  $\delta \approx 100$ . If  $\alpha$  were equal to zero, the curve would be Lorentzian in shape. However, there are fine-structure features due to the presence of the  $\mu$  component of the field. One is a sharp peak at  $\delta=96.55$ , which corresponds to the absorption of two  $\mu$ -type pho-

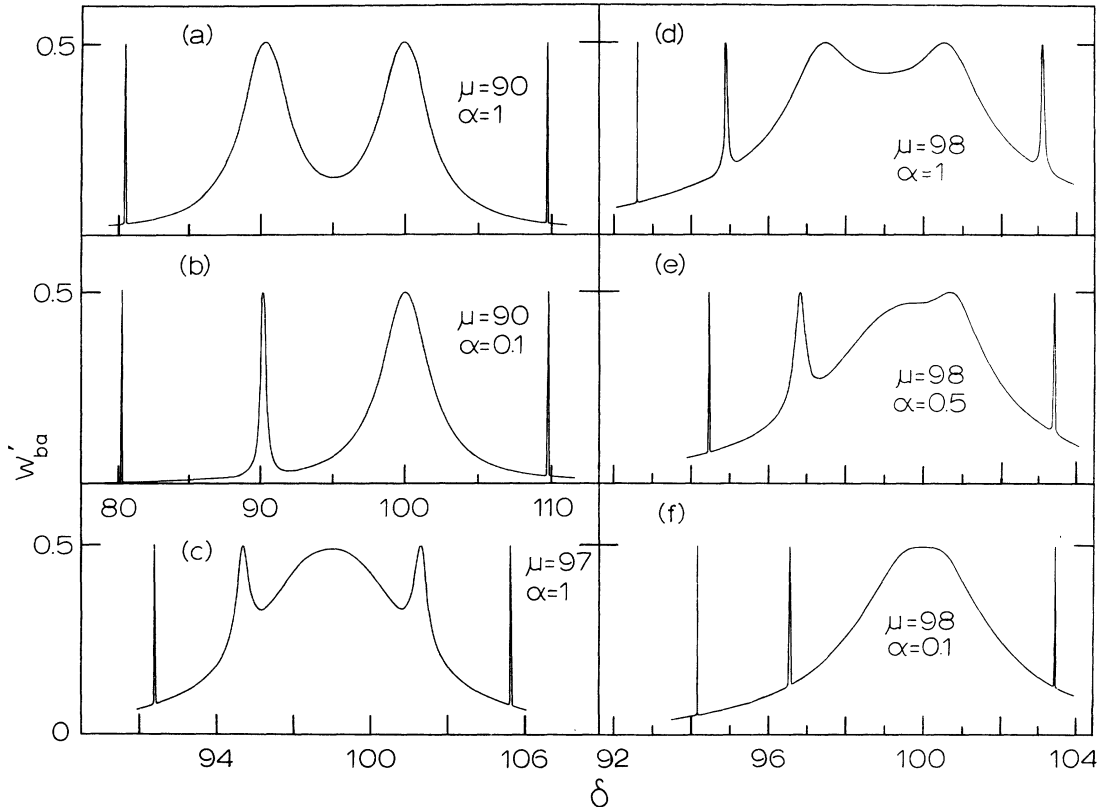


FIG. 8. Transition probability  $W'_{ba}$  as a function of  $\delta$  for the case  $\lambda=100$ .

tons and the emission of one  $\lambda$ -type photon. The frequency is substantially shifted from the value  $\delta = 2\mu - \lambda = 96$  because the system is being strongly driven by the  $\lambda$  field. An even sharper feature occurs at  $\delta = 103.45$ , identified with a multiphoton transition  $3\lambda - 2\mu$ . The features due to absorption of single  $\mu$ -type and single  $\lambda$ -type photons, as well as that due to the multiphoton process of type  $2\lambda - \mu$  are all superimposed in the central broad peak. The case  $\mu = 90$  and  $\alpha = 0.1$  with  $\lambda = 100$  is shown in Fig. 8(b); here the different components of the spectrum are clearly separated in frequency.

In all the cases mentioned above significant frequency shifts are present between the location of resonance peaks in  $W'_{ba}$  and the "expected" values,  $\delta = n\omega_\lambda - (n-1)\omega_\mu$ . This indicates that corrections will be necessary in deducing accurate atomic-energy-level spacings from double-resonance-type experiments, especially when high powers are used. These corrections can of course be calculated using the procedures of this paper provided that the transition dipole moments are known. Alternatively, a measurement of the intensity-dependent shift would yield a value of the dipole moment were this not already available.

In Fig. 9,  $W'_{ba}$  is plotted as a function of  $\alpha$  for the following choice of parameters:  $\lambda = 100$ ,  $\mu = 98$ , and  $\delta = 94.75$ . It is seen that the system is swept through a resonance at  $\delta \approx (3\mu - 2\lambda)$  simply by varying the intensity of the  $\mu$  component of the field by a relatively small amount.

The probability that the system is in the state  $|b\rangle$ , having started in  $|a\rangle$  at time  $t_0 = 0$ , has been calculated as a function of the time for a few cases. Curves for near-resonance and off-resonance cases are shown in Fig. 10:  $\delta = 99, 103$ , and  $103.12$ , with  $\lambda = 100$ ,  $\mu = 98$ , and  $\alpha = 1$ . When  $\delta = \frac{1}{2}(\lambda + \mu)$  (that is the first case), it turns out that the poles are located at  $\eta = \frac{1}{2}n(\lambda - \mu)$ ,  $n$  a positive or negative integer. Furthermore, only poles with  $n = 0, \pm 2$  contribute significantly to  $W_{ba}$  and one may express the probability in the form

$$W_{ba} \approx A + B \cos[\omega_c(\lambda - \mu)(t - t_0)] + C \cos[2\omega_c(\lambda - \mu)(t - t_0)]. \quad (3.24)$$

The constants  $A$ ,  $B$ , and  $C$  depend on the particular choice of  $\lambda - \mu$ . By contrast to (3.24), in the monochromatic case for the rotating-wave approximation the probability oscillates simply in a sinusoidal way [see Eq. (2.27) of I]. The third case plotted corresponds to the resonant condition of  $\delta \approx 3\lambda - 2\mu$ . It is seen that a much greater time is required to attain the condition  $W_{ba} = 1$  than for the case  $\delta = \frac{1}{2}(\lambda + \mu)$ .

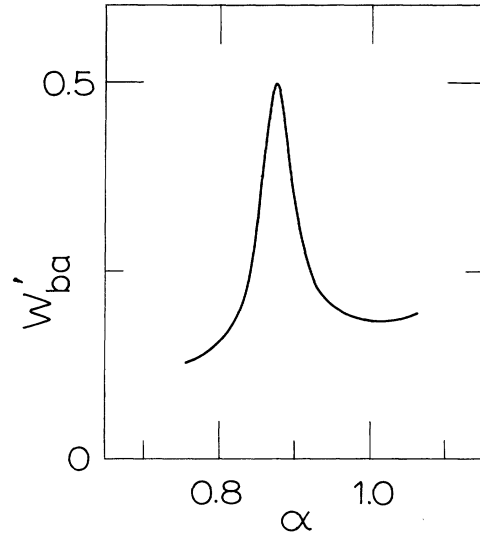


FIG. 9. Transition probability  $W'_{ba}$  as a function of  $\alpha$  for the case  $\lambda = 100$ ,  $\mu = 98$ , and  $\delta = 94.75$ .

#### B. Improvements on ladder approximation

When the frequency of the two components of the field is not close to resonance one is no longer justified in solving the problem by just making the ladder approximation. However, including more diagrams in the perturbation-theory approach leads to an unmanageable collection of products of propagators. One is then forced to turn to the Floquet's-theorem approach, taking into consideration more coefficients  $A_{nm}$  and  $B_{nm}$  than were in-

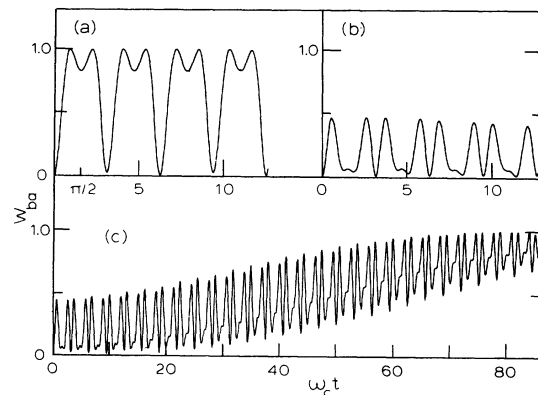


FIG. 10. Transition probability  $W_{ba}$  as a function of the reduced time  $\omega_c t$  for the case  $\lambda = 100$ ,  $\mu = 98$ , and  $\alpha = 1$ , with  $\delta = 99, 103, 103.12$  in (a), (b), and (c), respectively.

cluded in the ladder approximation.

In the recursion relations (3.2) every coefficient of type  $A$  or  $B$  is related to four coefficients of type  $B$  or  $A$ , respectively. This suggests that it may be convenient to assign the coefficients  $A$  and  $B$  to points in a square lattice in such a way that each coefficient has as nearest neighbors the four coefficients to which it is directly related by the recursion relations (3.2). The resulting diagram is shown in Fig. 11. We note that all the coefficients  $A_{nm}$  ( $B_{nm}$ ) lying along a diagonal line with slope  $-1$  are characterized by the same index  $r = m + n$ , the net number of emitted photons.

With reference to Fig. 11 the two cases so far treated can be discussed in the following terms. In the monochromatic case, that is  $\alpha = 0$ , the only nonzero coefficients lie in a vertical line through  $A_{00}$ . A given coefficient is hence connected only to two neighbors and a solution is readily obtained. In the more restricted case of the rotating-wave approximation all coefficients except  $A_{00}$  and  $B_{10}$  are neglected. In the ladder approximation to the bichromatic case only the central diagonal section of the array, where  $r = 0$  and  $r = 1$ , is taken into account. In this case again any point has only two nearest neighbors and consequently a relatively simple expression can be found for a given coefficient.

An obvious improvement to the ladder approximation is to include in the analysis coefficients with  $r = 2, 3, -1$ , and  $-2$ , that is, coefficients along diagonals parallel to the "ladder" diagonal.

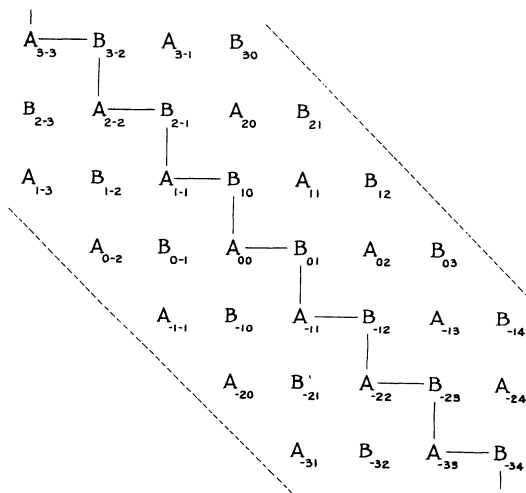


FIG. 11. Coefficients  $A_{nm}$  and  $B_{nm}$  laid out on a square lattice. In the ladder approximation only those coefficients joined by the solid lines are taken into account. The dashed lines mark the boundary of the array used in the calculations with  $\lambda = 100$  and  $\mu = 90$ .

In terms of perturbation theory this choice of coefficients is equivalent to including propagators (in  $\mathcal{G}_{ab}$ ) in which as many as three successive emissions, or two successive absorptions of either  $\lambda$ - or  $\mu$ -type photons take place. If  $\alpha$  were equal to zero this approximation would lead to the zero-photon propagator

$$\mathcal{G}_{aa}^{(0)} = \left[ \eta - i\epsilon - \left( \frac{1}{\eta' - \lambda - i\epsilon} - \frac{1}{\eta - 2\lambda - i\epsilon} - \frac{1}{\eta' - 3\lambda - i\epsilon} \right) - \left( \frac{1}{\eta' + \lambda - i\epsilon} - \frac{1}{\eta + 2\lambda - i\epsilon} \right) \right]^{-1}. \quad (3.25)$$

This is a very good approximation for  $\delta \approx 100$  or greater, but it would become questionable if  $\lambda$  were of the order of 10. It is of course necessary to extend the diagonal array of coefficients only a finite distance away from  $A_{00}$ . In practice one terminates it at the coefficients  $A_{N,-N}$  and  $A_{-N,N}$ , where  $N$  is determined empirically.

With this selection of nonzero coefficients it is possible to express all of them in terms of the coefficients  $A_{n,-n}$ . One then must solve numerically  $2N$  simultaneous equations for the ratios  $A_{n,-n}/A_{00}$ . From these solutions one calculates the coefficients  $B_{01}$ ,  $B_{0,-1}$ ,  $B_{10}$ , and  $B_{-10}$ , from which  $\mathcal{G}_{aa}^{(0,0)}$  may be evaluated and its poles and residues deduced. Since all the coefficients in the chosen array may now be calculated,  $\mathcal{G}_{aa}^{(N,M)}$  and  $\mathcal{G}_{ab}^{(N,M)}$  are known through Eqs. (3.5).

### 1. Numerical examples

The foregoing procedure was used to calculate the Green's function for the following values of the parameters:  $\lambda = 100$ ,  $\mu = 98$ ,  $\alpha = 1$ ;  $\lambda = 100$ ,  $\mu = 97$ ,  $\alpha = 1$ ;  $\lambda = 100$ ,  $\mu = 90$ ,  $\alpha = 1 - 0.1$ . From these Green's functions the probability that the system makes a transition from state  $|a\rangle$  to state  $|b\rangle$  was evaluated, and two of the results have already been presented in Figs. 8(a) and 8(b). The difference between  $W'_{ba}$  calculated in the ladder approximation and  $W_{ba}$  calculated using this procedure was small in the cases  $\mu = 98$  and  $\mu = 97$ , and was essentially confined to a frequency shift in the location of the sharp maxima due to multiphoton transitions. The Green's functions were also used to calculate the probability of scattering, to be discussed in Sec. III B 2.

In comparison to the ladder approximation, this more complete calculation reveals the existence of additional poles shifted away from the ones given by Eq. (3.21) by  $2m\mu$ . That is,

$$P_{mni}^a = -\frac{1}{2}\gamma + l\xi + n\Delta + 2m\mu. \quad (3.26)$$

These additional poles are to be expected, of course, on the basis of the form of the postulated wave function (3.1). Corresponding to each

pole of  $g_{ij}^{(N,M)}$  is a residue denoted by the symbol  $R(ij|mnlNM)$ , and the Green's-function operator equals

$$G_{ij} = -|i\rangle\langle j| e^{-i\omega_i(t-t_0)} \frac{1}{2\pi} \int d\eta e^{i\eta\omega_c(t-t_0)} \times \sum_{m,\dots,M} \frac{R(ij|mnlNM)}{\eta - P_{mnl}^i - i\epsilon} e^{i(N\omega_\lambda + M\omega_\mu)t_0}. \quad (3.27)$$

In practice only one pole need be located by solving Eq. (3.3), all the rest following by the application of the above relation (3.26). The accuracy of the numerical results was tested in the same way as for the ladder approximation to the Green's function.

## 2. Scattering

In the discussion of the Green's-function operator in the previous sections the language of photon emission or absorption has been introduced as a matter of convenience; these photons are emitted into and absorbed from the applied field and are hence not observable. We would now like to calculate the probability that the system emits photons accessible to an observer, that is, the probability of photon scattering.

$$S_{pq} = i \langle \kappa | \langle p | e^{i\omega_p t} \Delta G e^{-i\omega_q t_0} | q \rangle | 0 \rangle = \left( \frac{2\omega_\kappa}{V} \right)^{1/2} e^{i(\omega_{pq} + \omega_\kappa)t_0} \sum_{k,k'} (\vec{d}_{kk'} \cdot \vec{\epsilon}_\kappa) \sum_{m,n,\dots,M'} R(pk|mnlNM) R(k'q|m'n'l'N'M') \times \exp i \left\{ \left[ (N+N')\omega_\lambda + (M+M')\omega_\mu \right] t_0 + \frac{1}{2}\omega_c \left[ P_{mnl}^p + P_{m'n'l'}^{k'} + (1/\omega_c)(\omega_{pk'} + N\omega_\lambda + M\omega_\mu + \omega_\kappa) \right] (t-t_0) \right\} \times \frac{\sin(\omega_c/2) \left[ P_{mnl}^p - P_{m'n'l'}^{k'} - (1/\omega_c)(\omega_{pk'} + N\omega_\lambda + M\omega_\mu + \omega_\kappa) \right] (t-t_0)}{\omega_c \left[ P_{mnl}^p - P_{m'n'l'}^{k'} - (1/\omega_c)(\omega_{pk'} + N\omega_\lambda + M\omega_\mu + \omega_\kappa) \right]}. \quad (3.30)$$

To obtain (3.30) use has been made of the definition of  $G^+$ , Eq. (2.4), and the relation (3.27) for  $G_{ij}$ .

The cross section for scattering will be proportional to  $|S_{pq}|^2$ . In order that it be independent of the initial and final time it is clear that restrictions on the sums over the indices in (3.30) will be necessary. Furthermore, for  $t-t_0$  large, the frequency of the emitted photon is well defined and equal to

$$\omega_\kappa = \omega_c (P_{mnl}^p - P_{m'n'l'}^{k'}) - \omega_{pk'} - N\omega_\lambda - M\omega_\mu. \quad (3.31)$$

$$\sigma(\omega_\kappa) = \frac{V}{(2\pi)^3 (I_\lambda/\omega_\lambda + I_\mu/\omega_\mu)} \int d^3\kappa \left[ \frac{d}{dt} (|S_{ba}|^2 + |S_{aa}|^2) \right] = A_\kappa \sum_{j \neq k} \sum_{j' \neq k'} \sum_{x,\dots,x'''} [R(aj|x) R(ka|x') R(aj'|x'') R(k'a|x''') + R(bj|x) R(ka|x') R(bj'|x'') R(k'a|x''')]. \quad (3.33)$$

In (3.33) the symbols  $x, x',$  etc., have been introduced to stand for the set of five indices  $mnlNM$ , required to completely specify a residue. The prime on the sum over the indices  $x, x',$  etc.,

The two-level system is coupled to a quantized field via the electric dipole moment. The part of the interaction Hamiltonian effective in photon emission may be written

$$H_I = i(2V)^{-1/2} \sum_\nu \vec{d} \cdot \vec{\epsilon}_\nu \omega_\nu^{1/2} b_\nu^\dagger e^{i\omega_\nu t}, \quad (3.28)$$

where  $\nu$  specifies a field mode of frequency  $\omega_\nu$  and momentum  $\vec{k}_\nu$ , and  $\vec{\epsilon}_\nu$  is the polarization vector.  $b_\nu^\dagger$  is the creation operator for the field and  $V$  the quantization volume. The units are chosen so that  $c = \hbar = 1$ .

This interaction potential introduces a first-order change in the Green's-function operator equal to

$$\Delta G = \int dt' G^+(t-t') H_I(t') G^+(t'-t_0), \quad (3.29)$$

where  $G^+$  is the Green's-function operator satisfying Eq. (2.1). The amplitude of a transition in which the two-level system immersed in the classical field at time  $t=t_0$  goes from the state  $|q\rangle$  to the state  $|p\rangle$  at the time  $t$  and the quantized field goes from the vacuum state  $|0\rangle$  to the one-photon state  $|\kappa\rangle$  equals,

Introducing the pole locations (3.26) one sees that possible values for  $\omega_\kappa$  are,

$$\omega_\kappa = (2r+1)\omega_{\lambda(\mu)} + s(\omega_\lambda - \omega_\mu) + v\xi\omega_c, \quad (3.32)$$

where  $r$  and  $s$  are positive or negative integers and  $v$  has the values  $0, \pm 2$ .

Assuming the system to be initially in the state  $|a\rangle$ , the cross section for emitting a photon of frequency  $\omega_\kappa$  without regard to the final atomic state equals

means that restrictions have been imposed on the indices  $m, n, l, m', n',$  etc., so that  $\sigma$  is stationary, and furthermore, so that  $\omega_\kappa$  has the desired value.<sup>12</sup> The quantity  $A_\kappa$  equals

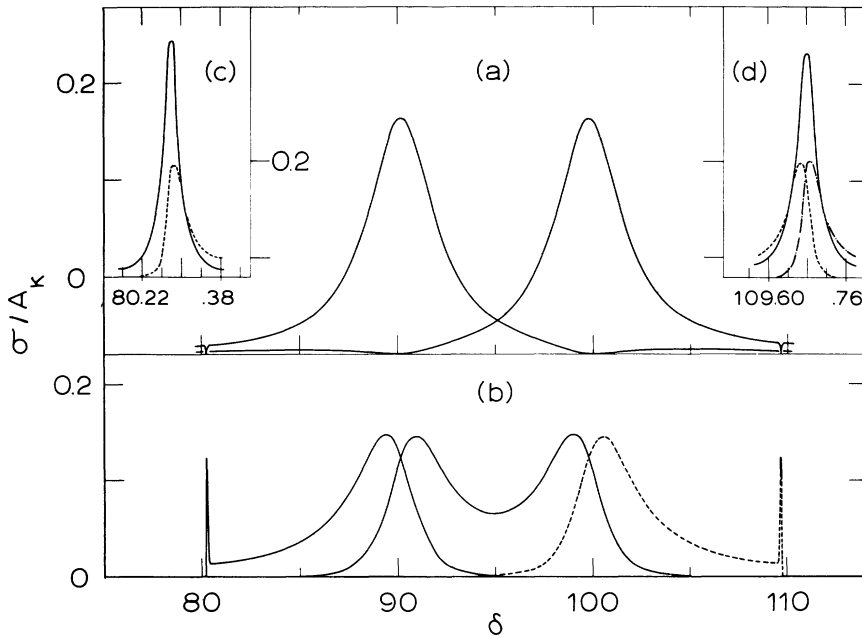


FIG. 12. Scattering cross section (divided by  $A_k$ ) as a function of  $\delta$ , for the case  $\lambda=100$ ,  $\mu=90$ , and  $\alpha=1$ . (a) Scattering at  $\omega_k = \omega_\mu$ , and  $\omega_\lambda$ . (b) Solid curves, for scattering into the satellites of  $\omega_\mu$ :  $\omega_k = \omega_\mu \pm 2\zeta\omega_c$ . Dashed curve, for the satellite at frequency  $\omega_k = 2\omega_\lambda - \omega_\mu - 2\zeta\omega_c$ . (c) Scattering at  $\omega_k = 2\omega_\mu - \omega_\lambda$  (solid curve) and  $\omega_k = \omega_\mu - 2\zeta\omega_c$  (dashed curve). (d) Scattering at  $\omega_k = 2\omega_\lambda - \omega_\mu$  (solid curve),  $\omega_k = 2\omega_\lambda - \omega_\mu + 2\zeta\omega_c$  (dashed curve), and  $\omega_k = 2\omega_\lambda - \omega_\mu - 2\zeta\omega_c$  (dot-dashed curve).

$$A_k = \frac{\pi \omega_k^3}{(2\pi)^3 (I_\lambda/\omega_\lambda + I_\mu/\omega_\mu)} \int d\Omega_k (\vec{d}_{ab} \cdot \vec{e}_k)^2, \quad (3.34)$$

where  $I_\lambda$  and  $I_\mu$  are the intensity of the  $\lambda$  and  $\mu$  components of the bichromatic field, and  $d\Omega_k$  is an element of solid angle into which the photon is emitted.

The cross section for scattering at  $\omega_k = \omega_\mu$ ,  $\omega_\lambda$ ,  $2\omega_\lambda - \omega_\mu$ , and values shifted from these by  $\pm 2\zeta$  has been worked out numerically for the specific case  $\lambda=100$ ,  $\mu=90$ , and  $\alpha=1$ . These results are presented in Fig. 12. In Fig. 12(a) is plotted, as a function of  $\delta$ , the cross section for Rayleigh scattering, that is, for scattering at the frequency of the components of the incident field. These curves have maxima for  $\omega_{ba}$  near  $\omega_\mu$  and  $\omega_\lambda$ , frequency shifts present being similar to those exhibited by  $W'_{ba}$ . It may be noticed, in addition, that the cross section for scattering at  $\omega_k = \omega_\mu$  shows minima near  $\omega_{ba} = 100$  and  $80.22$ , while that for scattering at  $\omega_k = \omega_\lambda$  has minima near  $\omega_{ba} = 90$  and  $\omega_{ba} = 109.74$ . At these values of  $\omega_{ba}$  the scattering cross section is large for other values of the frequency  $\omega_k$ , for example, for  $\omega_k = \omega_\mu$  and  $2\omega_\lambda - \omega_\mu$ , respectively, in the latter case.

In Fig. 12(b) is shown the cross section for production of the satellite lines at  $\omega_k = \omega_\mu + 2\zeta$ ,  $\omega_\mu - 2\zeta$ , and  $2\omega_\lambda - \omega_\mu - 2\zeta$ . The maximum cross section for these features is approximately half the maximum cross section for the Rayleigh lines. In the insets, Figs. 12(c) and 12(d), are shown details of the cross section on an expanded  $\omega_{ba}$

scale. Fig. 12(c) corresponds to scattering near  $\omega_k = 2\omega_\mu - \omega_\lambda$ . Only one satellite is shown; the other, which would belong to  $3\omega_\mu - 2\omega_\lambda$  was not calculated. Fig. 12(d) corresponds to scattering near  $\omega_k = 2\omega_\lambda - \omega_\mu$ . The satellites are similar in behavior to the satellites in the monochromatic case, discussed in I. The frequency of all the satellite lines as a function of  $\omega_{ba}$  is shown in Fig.

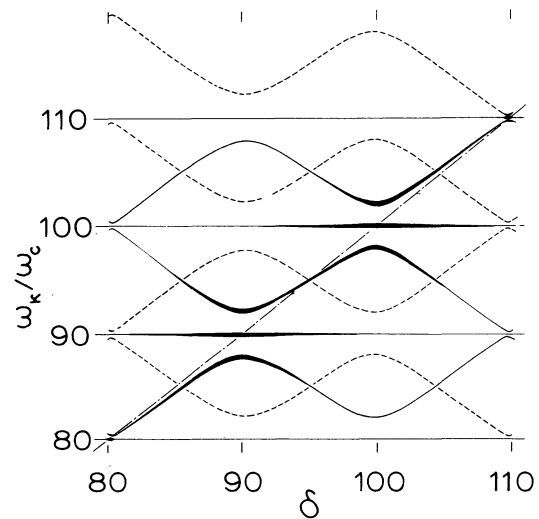


FIG. 13. Frequency of the scattered radiation as a function of  $\delta$  for the case  $\lambda=100$ ,  $\mu=90$  and  $\alpha=1$ . Those components of the spectrum which are most intense are indicated by heavier weight lines. The dot-dashed diagonal line is the curve  $\omega_k = \omega_{ba}$ .

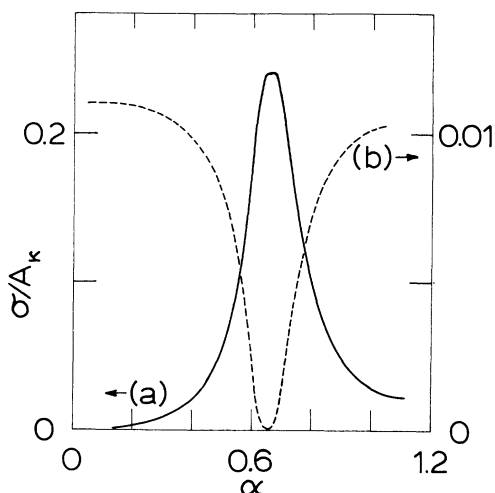


FIG. 14. Cross section for scattering as a function of  $\alpha$  for the case  $\lambda=100$ ,  $\mu=90$ ,  $\delta=109.74$ , and (a)  $\omega_\kappa = 2\omega_\lambda - \omega_\mu$ ; (b)  $\omega_\kappa = \omega_\lambda$ .

13. The highest intensity features have been indicated with a line of heavy weight, while the weak features are indicated with dotted lines. Roughly speaking, the most intense scattering takes place at the frequency  $\omega_\kappa$  which is closest to  $\omega_{ba}$ .

The frequency  $\omega_{ba}$  at which maxima occur in  $\sigma$  depends on the intensity of the  $\mu$  component of the

field. This is illustrated in Fig. 14(a), which is a plot of the scattering cross section at  $\omega_\kappa = 2\omega_\lambda - \omega_\mu$  as a function of  $\alpha$  for the fixed value  $\delta = 109.74$ . It is seen that by varying the intensity of the  $\mu$  component the system can be caused to pass through a resonance. In Fig. 14(b) the cross section for scattering at  $\omega_\kappa = \omega_\lambda$  is also shown as a function of  $\alpha$  for the same value of  $\delta$ . It is seen that this cross section passes through a minimum, and for  $\alpha = 0.65$  the system would not scatter any photons of frequency  $\omega_\lambda$ . This rapid change in the scattering cross section as a function of  $\alpha$  is one of the most interesting results of this investigation, because it implies that the index of refraction of a gas of these two-level atoms may be made strongly intensity dependent. That is, the index of refraction at frequency  $\omega_\lambda$ , say, can be made sensitive to the intensity of the  $\mu$  component of the field by appropriate choice of all the system's parameters. In practical terms, this means that one could phase modulate the  $\lambda$  component of the field by intensity modulating the  $\mu$  component. In the example chosen, the two components of the field have a similar frequency, but an analogous effect would exist if, for example, the  $\lambda$  component were radiation from an infrared laser and the  $\mu$  component were a microwave field. Experiments are underway to investigate these effects.

<sup>1</sup>R. Gush and H. P. Gush, *Phys. Rev. A* **6**, 129 (1972) (and references therein), to be referred to as I in the text.

<sup>2</sup>C. S. Chang and P. Stehle, *Phys. Rev. A* **4**, 641 (1971).

<sup>3</sup>B. R. Mollow, *Phys. Rev. A* **5**, 2217 (1972).

<sup>4</sup>S. Swain, *J. Phys. A* **5**, 1587 (1972).

<sup>5</sup>D. F. Walls, *J. Phys. A* **4**, 638 (1971).

<sup>6</sup>F. Chiarini, M. Martinelli, S. Santucci, and P. Bucci, *Phys. Rev. A* **6**, 1300 (1972).

<sup>7</sup>T. Oka and T. Shimizu, *Appl. Phys. Lett.* **19**, 88 (1971); S. M. Freund, J. W. C. Johns, A. R. W. McKellar, and T. Oka, *J. Chem. Phys.* **59**, 3445 (1973).

<sup>8</sup>E. L. Ince, *Ordinary Differential Equations* (Longmans, Green and Co., New York, 1927).

<sup>9</sup>S. H. Autler and C. H. Townes, *Phys. Rev.* **100**, 703

(1955).

<sup>10</sup>The spontaneous emission of a single, excited two-level system into a quantized field of two modes, initially empty, has been treated by S. Swain (see Ref. 4). In this case only the diagrams just mentioned are important. He obtains an expression for the probability of the system's being in the excited state as a function of the time, which is the same as one would obtain using (3.12) as a Green's function.

<sup>11</sup>The choice of values of the parameters  $\lambda$  and  $\mu$  is, of course, arbitrary. We have chosen the smallest values of both (that is, the highest intensity case) for which this treatment can be expected to be valid.

<sup>12</sup>For more details of the type of restrictions required, see Ref. 1.